J. Physiol. (1977), **268**, *pp.* 177–210
With 14 *text-figures*
Printed in Great Britain

RECONSTRUCTION OF THE ACTION POTENTIAL OF VENTRICULAR MYOCARDIAL FIBRES

BY G. W. BEELER* AND H. REUTER†

*From the *Department of Physiology and Biophysics, Mayo Clinic, Rochester, Minnesota 55901, U.S.A., and the †Department of Pharmacology, University of Bern, 3010 Bern, Switzerland*

(*Received 14 September 1976*)

SUMMARY

1. A mathematical model of membrane action potentials of mammalian ventricular myocardial fibres is described. The reconstruction model is based as closely as possible on ionic currents which have been measured by the voltage-clamp method.

2. Four individual components of ionic current were formulated mathematically in terms of Hodgkin–Huxley type equations. The model incorporates two voltage- and time-dependent inward currents, the excitatory inward sodium current, i_{Na}, and a secondary or slow inward current, i_s, primarily carried by calcium ions. A time-independent outward potassium current, i_{K_1}, exhibiting inward-going rectification, and a voltage- and time-dependent outward current, i_{x_1}, primarily carried by potassium ions, are further elements of the model.

3. The i_{Na} is primarily responsible for the rapid upstroke of the action potential, while the other current components determine the configuration of the plateau of the action potential and the re-polarization phase. The relative importance of inactivation of i_s and of activation of i_{x_1} for termination of the plateau is evaluated by the model.

4. Experimental phenomena like slow recovery of the sodium system from inactivation, frequency dependence of the action potential duration, all-or-nothing re-polarization, membrane oscillations are adequately described by the model.

5. Possible inadequacies and shortcomings of the model are discussed.

INTRODUCTION

The application of voltage-clamp techniques to the study of the membrane ionic currents in heart muscle, has shown that the quantitative analysis of the various ionic current components underlying cardiac

action potential is much more complex than in nerve (for review see Trautwein, 1973; McAllister, Noble & Tsien, 1975). While there is a great deal of agreement on the main experimental results, there remain many areas of uncertainty relative to the kinetics of the dynamic currents. A complete kinetic analysis of all dynamic ionic currents in cardiac muscle has not been possible because of the morphological complexity of the preparations and technical limitations of the voltage-clamp methods. Nevertheless, several quantitative studies which provide a better understanding of membrane ionic currents in cardiac muscle have emerged from the application of the voltage-clamp.

This paper is a report of a numerical simulation of the ventricular myocardial action potential which seeks to incorporate the majority of the experimental evidence. In a sense, it forms a companion presentation to the recent publication of McAllister *et al.* (1975) on a numerical reconstruction of the cardiac Purkinje fibre action potential. There are sufficiently many and important differences between these two types of cardiac tissue, both functionally and experimentally, that a more or less complete picture of membrane ionic currents in the myocardium must include both simulations.

The primary emphasis in this paper will be on the role of the slow inward current (i_s) mainly carried by calcium ions which plays a dominant part in the creation of the myocardial action potential plateau, and which forms an intimate link between electrical events at the membrane and the contractile responses of the cell (cf. reviews Bassingthwaighte & Reuter, 1972; Reuter, 1973, 1974; Noble, 1975).

The model presented here relies on published data from various laboratories. To the degree that the model has permitted the definition of additional experiments that might elucidate a given characteristic of the membrane ionic currents, we have attempted to perform some of those experiments, and a limited amount of experimental data is incorporated in this paper for corroborative evidence. The simulation is confined to uniform 'membrane action potentials', and therefore does not define conditions for propagation of the action potential.

METHODS

Experimental. The experimental data that are presented in this paper were all achieved with the single sucrose-gap voltage-clamp technique (Beeler & Reuter, 1970*a*). This experimental approach has been modified in two ways since our original report. Firstly, we have adopted a better bath grounding system, wherein the test-bath is grounded through the summing junction of an operational amplifier (New & Trautwein, 1972). Secondly, electronic switches permit the investigator to produce a transition from current-clamp to voltage-clamp mode within 20 μsec. Thus he may produce a voltage-clamp at any time during a normal action potential

or conversely may release the preparation from the voltage-clamp at any time he desires.

Mathematical. The bulk of the material presented herein represents a numerical simulation of the action potential. This simulation is the result of the solution of a system of eight, first order, simultaneous, non-linear differential equations. The simulations were performed using a simulation system, Simcon (Anderson, Knopp & Bassingthwaighte, 1970), which operates on a Control Data Corporation 3500 computer. This system permits the investigator to interact with a numerical model written in FORTRAN from an on-line terminal. During the simulation, model results are plotted on an oscilloscope at the investigator's terminal and he has the ability to alter the model or the computational process during the simulation. Moreover, he controls the over-all characteristics of the model through the interactive entry of an array of up to 300 parameters which define the model. The results of each simulation are temporarily stored on magnetic disk and then may be replotted to form figures, such as are used in this paper, or may be listed for more detailed analysis.

The integration algorithm used to solve the differential equations is the Runge–Kutta–Merson algorithm (Lange, 1960). This algorithm uses five evaluations of the derivatives during each step of the integration, and produces both a result with fourth-order accuracy, and a prediction of truncation error. The truncation error estimate is used to control the step size of the integration procedure, in order to optimize the time required for solution against the accuracy of the solution.

Any integration algorithm which incorporates an estimate of error in order to control step size will have the maximum step size limited by the smallest time constant in the system being integrated. In the model presented here, the time constant for the activation of the sodium current is at least an order of magnitude faster than any of the other time constants within the system. Moreover, this parameter is in equilibrium with its steady-state value at all times except during the upstroke of the action potential. Therefore, an algorithm was devised which monitors both the difference between the value of this parameter and its steady-state value, and the instantaneous rate of change of the membrane potential. If at any time during the computation the parameter and its steady-state value differ by less than 0·004, and if the rate of change of the membrane potential is also less than 0·5 V/sec, then the algorithm ceases integrating this parameter. This increases integration speed in two ways. Firstly, the system is reduced to seven simultaneous differential equations, a relatively minor gain. More importantly, however, the time constant governing the step size of the integration becomes an order of magnitude larger. During the periods when this parameter is not being integrated, it is continually set to its steady-state value as determined by the membrane potential, and the rate of change of this parameter over the last integration step is monitored. If this rate of change exceeds 0·005/msec, then the parameter is 're-captured' and the system returns to integrating all parameters. Incorporation of this algorithm, permits about a twentyfold increase in computational speed for the over-all system, and a single action potential can be computed in about 40 sec.

Model program. The primary model is a single space-clamped patch of membrane which consists of a membrane capacity with four parallel current paths. Eight parameters must be integrated to produce a solution to this model. These are the membrane potential across the capacity, the intracellular calcium ion concentration as it is affected by i_s, and six activation or inactivation parameters for the various conductances. At each step in time, the Runge–Kutta–Merson integration algorithm establishes a set of values for the variables being integrated (initial conditions for the step) and provides these values: membrane potential, $[Ca]_i$, and six

conductance parameters; to a subprogram which computes the derivative for each integrated variable. During this process, the individual ionic currents are determined and summed along with any 'externally applied' current to arrive at the charging current for the membrane capacity, which then determines the derivative of the membrane potential.

Within this basic computational approach, three different forms of simulation are realized. The most common mode computes the action potential by starting the integration algorithm with a set of initial conditions, and allowing the program to proceed through subsequent integration steps. In the instance that a stimulus current is desired, the derivative subprogram adds this external current to the ionic currents during the appropriate time steps.

The second computational mode involves the simulation of an ideal voltage-clamp experiment. This is done by setting the membrane potential equal to the desired voltage-clamp stimulus. Computation is then reduced to the integration of the intracellular calcium ion concentration as it is altered by the i_s. In this mode the conductance parameters for all channels can be expressed as simple exponential functions and need not be integrated. The output in this instance is the sum of the ionic currents from the various channels.

The third mode is an alternate approach to the simulation of the voltage-clamp and incorporates the concept of an extracellular series resistance (Beeler & Reuter, 1970*a*). Here, the simulated voltage-clamp circuit controls the voltage across the series combination of the membrane patch and a series resistance, R_s. In this instance,

$$i_{\text{clamp}} = (V_{\text{clamp}} - V_{\text{membrane}})/R_s, \tag{1}$$

where V_{membrane} is the potential across the membrane patch. In order to simulate this circuit, the derivatives for all integrated parameters including the membrane potential are determined as if for an action potential, but at each integration step i_{clamp} is determined from eqn. (1) and applied as an 'external current' in the determination of the membrane potential derivative. This then forces the membrane potential to follow the desired clamp potential. The majority of voltage-clamp simulations presented in this paper were done with the latter approach using an R_s of 200 Ω.

THEORY

Basis for the model

General

As noted, the general form of the model is that of a space-clamped patch of membrane. The nominal area for this membrane is one square centimetre, but it should be recognized that the majority of experimental results on which this work is based have not provided an accurate estimate of membrane area. The membrane capacity utilized in this model is set at 1 μF/cm^2 which is close to experimental values in the literature (Weidmann, 1970), and to the generally accepted value for the capacity of biological membranes. All ionic current densities refer to 1 cm^2. The scaling of the individual ionic currents is chosen to provide current–voltage relationships which match the best estimates obtained experimentally, but which, when taken together, produce an acceptable shape for the myocardial action potential. It should be noted, that the exact

TABLE 1. *A*, equations and values which define currents

$$i_{K_1} = 0{\cdot}35\{4(\exp[0{\cdot}04(V_m+85)]-1)/(\exp[0{\cdot}08(V_m+53)]+\exp[0{\cdot}04(V_m+53)]) + 0{\cdot}2(V_m+23)/(1-\exp[-0{\cdot}04(V_m+23)])\}. \quad (2)$$

$$\overline{i_{x_1}} = i_{x_1}.x_1, \quad (3)$$

where $$\overline{i_{x_1}} = 0{\cdot}8(\exp[0{\cdot}04(V_m+77)]-1)/\exp[0{\cdot}04(V_m+35)]. \quad (4)$$

$$i_{Na} = (\overline{g_{Na}}.m^3.h.j+g_{NaC})(V_m-E_{Na}), \quad (5)$$

where $\overline{g_{Na}} = 4$, $g_{NaC} = 0{\cdot}003$, and $E_{Na} = 50$.

$$i_s = \overline{g_s}.d.f.(V_m-E_s), \quad (6)$$

where $g_s = 0{\cdot}09$, and

$$E_s = -82{\cdot}3-13{\cdot}0287\ln[Ca]_i. \quad (7)$$

In the equations above, currents (i) are in μA/cm^2, voltages (E, V) are in mV, conductances (g) are in mmho/cm^2, and x_1, m, h, j, d and f are dimensionless. Membrane potential, V_m, is taken as inside potential minus outside potential.

B, equations defining time derivatives in model

$$dV_m/dt = -(1/C_m)(i_{K_1}+i_{x_1}+i_{Na}+i_{Ca}-i_{external}), \quad (8)$$

where $C_m = 1$.

$$d[Ca]_i/dt = -10^{-7}.i_s+0{\cdot}07(10^{-7}-[Ca]_i). \quad (9)$$

$$dy/dt = (y_\infty-y)/\tau_y, \quad (10)$$

where $$\tau_y = 1/(\alpha_y+\beta_y), \quad (11)$$

and $$y_\infty = \alpha_y/(\alpha_y+\beta_y). \quad (12)$$

In equations of *B*, times (t, τ) are in msec, membrane capacity is in μF/cm^2, $[Ca]_i$ is in mole/l, rate constants (α, β) are in msec^{-1}, and remaining units are as in *A*. Eqns. 10–12 show the method of computing the dimensionless conductance parameters using y to represent such a parameter.

C, defining function and values for rate constants (α or β)

$$\alpha = (C_1\exp[C_2(V_m+C_3)]+C_4(V_m+C_5))/(\exp[C_6(V_m+C_3)]+C_7). \quad (13)$$

Rate constant	C_1	C_2	C_3	C_4	C_5	C_6	C_7
(msec^{-1})	(msec^{-1})	(mV^{-1})	(mV)	((mV.msec)$^{-1}$)	(mV)	(mV^{-1})	
α_{x_1}	0·0005	0·083	50	0	0	0·057	1
β_{x_1}	0·0013	−0·06	20	0	0	−0·04	1
α_m	0	0	47	−1	47	−0·1	−1
β_m	40	−0·056	72	0	0	0	0
α_h	0·126	−0·25	77	0	0	0	0
β_h	1·7	0	22·5	0	0	−0·082	1
α_j	0·055	−0·25	78	0	0	−0·2	1
β_j	0·3	0	32	0	0	−0·1	1
α_d	0·095	−0·01	−5	0	0	−0·072	1
β_d	0·07	−0·017	44	0	0	0·05	1
α_f	0·012	−0·008	28	0	0	0·15	1
β_f	0·0065	−0·02	30	0	0	−0·2	1

value of the membrane capacity has little effect on the over-all shape of the computed action potential, with the sole exception of the rapid upstroke. During the other phases of the action potential, the shape is primarily determined by the time constants of the dynamic ionic currents.

At various times, experimental evidence has been presented to postulate a total of eight different ionic conductance components in various cardiac muscle preparations (Trautwein, 1973). The model presented here incorporates only four of those components. These include: an initial fast inward current carried primarily by sodium, i_{Na}; a secondary or slow inward current, i_s, carried mainly but not exclusively by calcium ions; a time-activated outward current designated i_{x_1}; and a time-independent potassium outward current designated i_{K_1}. The rationale for the omission of the other currents will be presented in the sections to follow.

The complete set of equations and constants that define the model are given in Table 1. The general formulation for the ionic currents follows the concepts introduced by Hodgkin & Huxley (1952). Eqn. (6) is an example of a linear current term. When all slow inward current pathways are open or fully activated, i_s is determined by the linear current–voltage relation: $\overline{g_s}(V_m - E_s)$ (Reuter, 1973; Reuter & Scholz, 1976). At any point in time, however, only a fraction of the pathways are open, and the dimensionless conductance parameters d and f express the degree of activation and inactivation of this current. These parameters are functions of both membrane potential, V_m, and time. Investigations of the outward currents in Purkinje fibres have shown that when fully activated these currents have a non-linear, rectifying, current–voltage relationship. In order to characterize these currents, McAllister *et al.* (1975) adopted a formulation that is analogous to the linear case. This is shown in eqn. (3), where the non-linear current–voltage relation for the fully activated state, i_{x_1}, is multiplied by the dimensionless activation parameter, x_1.

The formulation for the time and voltage dependence of the activation parameters follows the approach first proposed by Hodgkin & Huxley (1952). With this approach, one defines a steady-state value for each activation parameter, which value varies between 0 and 1 over the voltage range of interest. This is referred to as the steady-state curve. The second potential dependent parameter directly related to the activation parameter is its time constant as a function of membrane potential. Utilizing these two factors, the rate of change of the activation parameter at any given moment is expressed by eqn. (10). In order to define the values of the steady-state curve, y_∞, and the time constant curve, τ_y, use is made of two rate-constant functions which are simply functions of membrane potential (Hodgkin & Huxley, 1952). These rate constants, α_y and β_y, then can be used to define the time constant curve and the steady-state

curve according to eqns. (11) and (12). In order to simplify the reporting of the actual values used in this model, we have expressed the alphas and betas entirely in terms of a generalized function, with eight defining coefficients. Table 1*C* gives the equation, and the defining coefficients for all rate constants.

Outward currents

The investigation of time-dependent outward currents in ventricular myocardium has been limited. This limitation arises primarily from the complication of the experimental method by the likely accumulation of potassium ions within the extracellular spaces of the myocardial muscle preparation during the long-lasting depolarizing voltage-clamps required for the analysis of these currents (McGuigan, 1974; Cleemann & Morad, 1976). Experimental work with the cardiac Purkinje fibre by Noble & Tsien (1968, 1969) has indicated the possible presence of three time-activated outward currents (i_{K_2}, i_{x_1} and i_{x_2}), and a time-independent potassium current exhibiting inward-going rectification (i_{K_1}). Available experimental evidence in working ventricular myocardium, however, can produce convincing evidence only for the presence of a single time-activated outward current, i_{x_1}, and for the background current, i_{K_1} (Beeler & Reuter, 1970*a*, and unpublished; McGuigan, 1974). The pace-maker potassium current, i_{K_2} (Noble & Tsien, 1968), seen in the cardiac Purkinje fibre, is probably not active in ventricular myocardium which does not normally exhibit spontaneous depolarization. The very slowly activated outward current, i_{x_2}, seen by Noble & Tsien (1969) is either not present in myocardial tissue, or is masked by the effects of extracellular potassium ion accumulation. Since the time constants of activation of i_{x_2} are extremely slow in comparison with a single action potential, this current component was not considered further in the present reconstruction. In an earlier version of our model, where i_{x_2} was included, we found that this current had a major influence on the shape of the action potential only during very rapid stimulation.

Although i_{x_1} is quite variable in size in ventricular myocardial fibres from different species, we have adopted the formulation of McAllister *et al.* (1975), for both the time-activated outward current i_{x_1} and the time-independent outward current i_{K_1}. These formulations are given in eqns. (2), (3), and (4) of Table 1, and the fully activated current–voltage relations are plotted in Fig. 1. In converting the formulae from those provided by McAllister *et al.* (1975), we re-scaled certain of the terms in the current–voltage relations and shifted these relations along the voltage axis. Although the general rationale behind this procedure was to account for the difference in extracellular potassium ion concentration between the

2·7 mM of their model and 5·4 mM which we seek to model, the ultimate criterion adopted by us was to match current–voltage relations seen in ventricular myocardium, and to realize a reasonable plateau and repolarization conformation for our computed action potential.

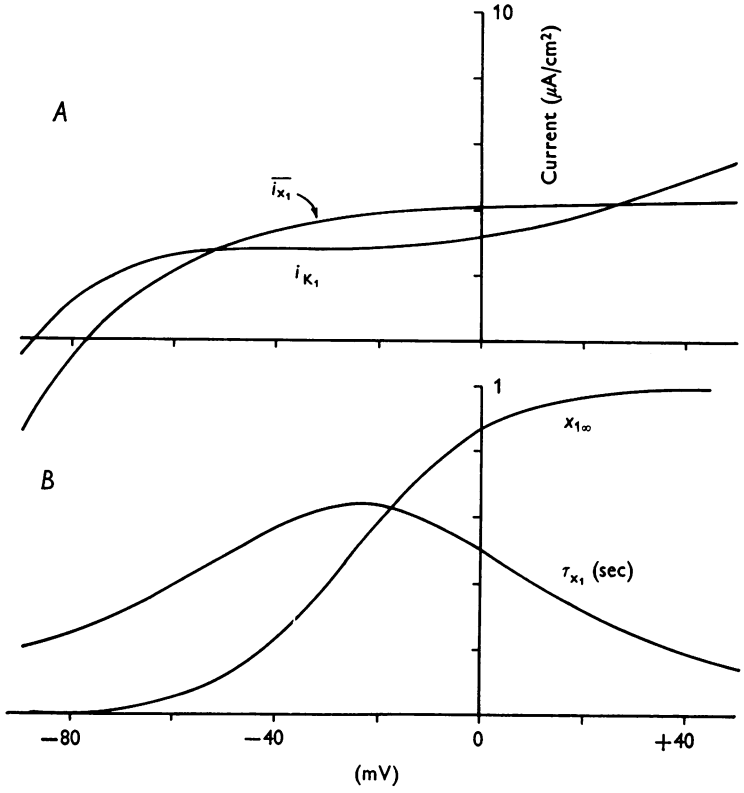

Fig. 1. *A*, the fully activated current–voltage relationship for potassium; $\overline{i_{x_1}}$ is the maximum current that can be obtained for the time-activated outward current; i_{K_1} is the background outward current which is present in the model. *B*, the steady-state value for the activation parameter, x_1, and values for τ_{x_1}. The ordinate is dimensionless for x_1 and is in sec for τ_{x_1}.

It should be noted that the first term in the i_{K_1} formulation can be taken to represent the residual effect of i_{K_2}, the pace-maker current (Noble & Tsien, 1968). Although there is no evidence that this current participates in a dynamic form in the normal myocardial action potential, it is conceivable that such a current is present in these preparations, but has an activation range sufficiently negative relative to the normal resting potential, that it does not participate dynamically in the formation of the action potential. Experimental evidence in potential ranges more negative than the resting potential has not been pursued in myocardial preparations, and therefore cannot assist in the resolution of this question.

The governing equations for the x_1 activation parameters as given in Table 1 are identical to those provided by McAllister *et al.* (1975). The steady-state values for the activation parameter, $x_{1\infty}$, and its time constants, τ_{x_1}, are plotted as a function of membrane potential in Fig. 1.

Inward sodium current

Experimental evidence is only partially available for the inward sodium current, i_{Na}, in cardiac muscle. We have chosen, in line with work in other tissues, to model the dynamic sodium inward current as a transient mechanism, wherein the equivalent conductance of the membrane for sodium is expressed as a maximum conductance multiplied by activation and inactivation parameters. The fundamental limitations of voltage-clamps applied to cardiac muscle have prevented the assessment of the activation kinetics of i_{Na} at normal temperatures. Therefore, like McAllister *et al.* (1975), we have adopted the formulation for the sodium activation parameter, m, determined for squid axon by Hodgkin & Huxley (1952).

The inactivation process for i_{Na} is somewhat more amenable to study using conditioning potentials produced by voltage-clamp, depolarization of the membrane with potassium chloride, or depolarization produced by the action potential. Indeed, the earliest works in this area by Weidmann (1955*a*) related to the inactivation process for the upstroke of the Purkinje fibre action potential. Beeler & Reuter (1970*a*) reported measurements of the steady-state inactivation curve, and much of this question has been re-investigated recently by Gettes & Reuter (1974). All of these experiments produce similar results in terms of the location and slope of the steady-state inactivation curve, h_∞. The evidence for the time constant for h, however, is not as strong. Voltage-clamp experiments would indicate that the inactivation process for i_{Na} must be complete within 10 msec or less at most potential levels and a similar conclusion can be drawn from the duration of the initial spike of the normal cardiac action potential. Haas, Kern, Einwächter & Tarr (1971) and Gettes & Reuter (1974), however, provided strong evidence to the effect that re-activation of i_{Na} proceeds at a much slower rate than inactivation. (Inactivation corresponds to changes in the parameter, h, from unity towards zero, or the shutting off of the sodium channel during depolarization, while re-activation corresponds to the return of this parameter to a unity value upon re-polarization as the sodium channel once again becomes available for activation.) The finding that the re-activation process is much slower than the inactivation process cannot be stimulated with a single, simple conductance parameter for inactivation. Therefore, following the suggestion by Haas *et al.* (1971) we have introduced in this model a second

inactivation parameter designated j, such that the formulation for i_{Na} becomes that of eqn. (5).

The steady-state inactivation parameter values j_∞ and h_∞ have identical dependence on membrane potential whereas their time constants are significantly different. The values for the rate constants for these two parameters, along with those for m are found in Table 1 and the steady-state values and time constants are plotted in Fig. 2. The rate constants

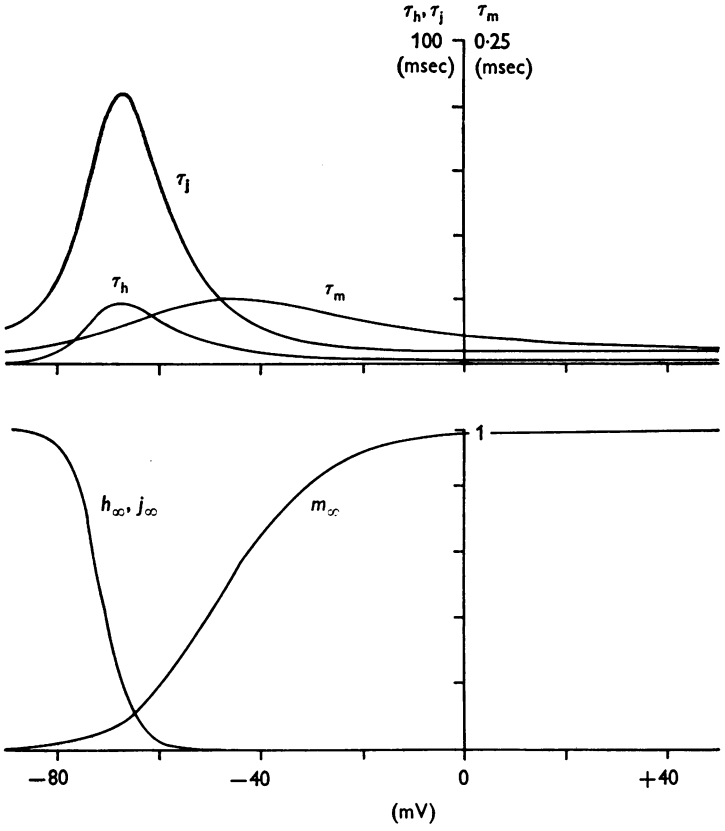

Fig. 2. *A*, time constants, and *B*, steady-state values for the activation (m_∞) and inactivation (h_∞, j_∞) parameters of the sodium conductance, g_{Na}, as functions of membrane potential.

for h were chosen by considering the effect of the time constant of h on the excitability of the model, and the shape of the spike of the computed action potential.

The values for τ_j were derived by matching the experimental results of Gettes & Reuter (1974) for potentials more negative than −60 mV and then 'bending' the τ_j curve to be roughly parallel to τ_h at more positive

potentials. The steady-state inactivation curves, j_∞ and h_∞, were matched to our earlier experimental results (Beeler & Reuter, 1970*a*; Gettes & Reuter, 1974). The values for the m, h and j steady-state functions and time constants, are plotted against membrane potential in Fig. 2.

The values in the model for the fully activated sodium conductance, $\overline{g_{Na}}$, for the background sodium conductance, $\overline{g_{NaC}}$, are 4·0 and 0·003 mmho/cm^2, respectively. These values, the h parameter time constants, and the absolute locations of the h_∞ and m_∞ curves were arrived at empirically by considering the interrelationships between the excitability of the model, the maximum upstroke velocity, and the peak and width of the action potential spike. The location of h_∞ on the voltage axis and its steepness agree with the experimental results by Gettes & Reuter (1974) but h_∞ is shifted by 5 mV towards negative potentials relative to the experimental results by Beeler & Reuter (1970*a*). The maximum amount of allowable cross-over between the steady-state curves for h_∞ and m_∞ is determined from the membrane current–voltage relationships, as no discernible 'notch' due to sodium has been observed experimentally in these curves. Once this separation is established, the relative location of both curves determines the threshold for the action potential. Finally, the maximum value of the action potential spike and the width of the spike are strongly determined by a combination of the inactivation time constant for sodium, τ_h, and the maximum conductance, $\overline{g_{Na}}$. We sought to model an excitation phase for the action potential which had a reasonably low threshold (-60 mV) achieved a maximum rate of rise of at least 115 V/sec, and which realized a peak at about $+30$ mV. The value for the steady-state sodium conductance, $\overline{g_{NaC}}$, was chosen to produce a steady sodium leak of about 0·4 μA/cm^2 at the resting potential. The sodium reversal potential, E_{Na}, was chosen in this model at 50 mV.

It should be noted that the formulation for sodium inactivation that we have adopted implies that the experimental approaches to measuring the steady-state inactivation curve with voltage-clamp or KCl depolarization will produce a curve that is the product of h_∞ and j_∞. It is worth considering, then, the difference between the curves h_∞ and $h_\infty{}^2$ (since j_∞ equals h_∞) that are likely to occur in these tissues. One means of expressing an inactivation curve, is with the following equation (Hodgkin & Huxley, 1952):

$$h_\infty = 1/(1+\exp[(V_m - V_h)/S]).$$

Here, the curve is characterized by a slope factor, S, and a half-point for the curve, V_h. The potential V_h is determined as that voltage at which h_∞ is 0·5. The slope factor, S, is then:

$$S = \left\{ -4 \frac{dh_\infty}{dV_m} \bigg| V_m = V_h \right\}^{-1}.$$

If the measured curve were indeed the square of the true inactivation curve, then the measurement of the slope, taken at the half-point of the squared curve, will

differ from the slope of the true inactivation curve by only 17%. The primary difference is that the half-point of the squared curve is shifted relative to that of the true curve. For example, in our earlier work we reported a V_h of -55 mV for the sodium inactivation curve, and a slope factor of 3 mV. If indeed we were measuring the square of an inactivation curve, then the true inactivation curve would have had a slope of 3·5 mV, and the true inactivation curve would have been located at about -52 mV. These differences are smaller than the experimental error in the estimates.

In arriving at the formulation used in this model, we fitted the rate constant equations for the sodium inactivation curves for both j_∞ and h_∞ to the experimental values that we had observed previously. For completeness, we have also calculated an equivalent set of rate constants which could be used under the assumption that our published figures represented an observation of $j_\infty . h_\infty$. This latter formulation produces no significant changes in the model.

As a further note, Gettes & Reuter (1974) discussed alternative formulations of i_{Na} activation and inactivation, for example, coupled activation–inactivation kinetics (Goldman, 1975). We have adopted the approach proposed by Haas *et al.* (1971) because of its simplicity and its similarity to the other activation and inactivation mechanisms used in this model. By adopting this approach we do not mean to imply a belief in one physical alternative over the other, but, rather, we recognize that present experimental evidence will not support the definition of a more elaborate scheme. The resolution of the question as to what sort of process is truly involved will require an experimental approach which provides extremely close control of the membrane potential during the flow of i_{Na} and realization of such a controlled cardiac muscle preparation may be unlikely with methods available today.

Slow inward current

The characterization of i_s has probably received more experimental attention than other current component. Available evidence from most laboratories indicates that in mammalian ventricular myocardium this current is carried predominantly by calcium ions when the preparations are superfused with physiological salt solutions containing calcium concentrations in the range 1–10 mM (for review see Reuter, 1973; Reuter & Scholz, 1976). This current is treated as a transient inward current, with simple activation and inactivation parameters multiplying a maximum conductance value (eqn. (6)). The activation parameter, d, and the inactivation parameter, f, cross-over strongly in the plateau range of potentials for the cardiac action potential (Fig. 3).

The shapes and locations of the activation and inactivation curves have been fairly well determined by G. W. Beeler and H. Reuter (unpublished), Bassingthwaighte & Reuter (1972), Reuter (1973, 1974), Trautwein, McDonald & Tripathi (1975), and Reuter & Scholz (1976). The curves used in defining this model represent a collation of the results obtained by Beeler & Reuter (1970*b*), Reuter (1973, 1974), and Gettes & Reuter (1974) and agree with recently published d_∞ and f_∞ curves of Trautwein *et al.* (1975) and Reuter & Scholz (1976). The steady-state activation and inactivation curves, and the time constants as functions of membrane

potential are shown in Fig. 3. Voltage-clamp studies indicate that the activation time constants, τ_d, for i_s reach a maximum of 40 msec at -20 mV (Reuter & Scholz, 1976).

The time constant curve for the inactivation parameter, f, represents a significant anomaly, when it is compared with the time constants determined for most other activation or inactivation parameters in excitable tissues. These curves have generally been found to be roughly bell-shaped, with the maximum value at approximately the half-point of the activation or inactivation parameter in question. The time constant for f,

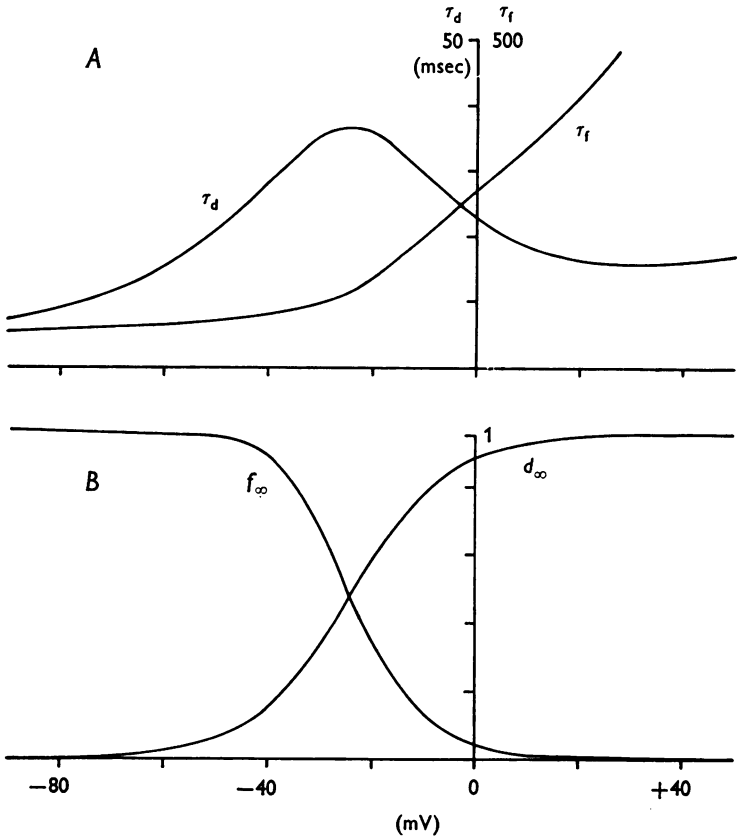

Fig. 3. *A*, time constants and *B*, steady-state values for the activation (d_∞) and inactivation (f_∞) parameters of the slow inward conductance, g_s, as functions of membrane potential.

however, appears from the best experimental evidence to be a continually increasing function of membrane potential. Although it is possible that this function might decrease at potentials more positive than $+15$ mV,

there is no experimental evidence for a maximum in the range of -20 mV where the f_∞ curve has its half-point. For cat papillary muscle New & Trautwein (1972) described a U-shaped relation between τ_f and membrane potential in the range -40 to $+40$ mV. Although their finding has been confirmed by Kohlhardt, Krause, Kübler & Herdey (1975), Trautwein *et al.* (1975) pointed out that the increase in τ_f at negative potentials is the result of an analytical error, and in principle they confirmed the shape of τ_f *vs.* V_m relationship obtained by Beeler & Reuter (1970*b*) and Gettes & Reuter (1974) (see also Reuter & Scholz, 1976). Another point of experimental discrepancy relates to the time constants of inactivation and of reactivation of i_s. While Gettes & Reuter (1974) did not find a major difference between these two time constants in pig and calf ventricular muscle, Kohlhardt *et al.* (1975) did describe such a difference in cat papillary muscle (cf. Reuter & Scholz, 1976).

Any attempt at modelling the influx of calcium into a muscle cell requires particular attention to the formulation adopted for the reversal potential for i_s. In order for the contractile proteins of this tissue to relax, the over-all intracellular calcium ion concentration at rest must be in the range between 1 and 3×10^{-7} M. If one then computes the influx of calcium from voltage-clamp experiments, or indeed from this model, the intracellular calcium ion concentration will increase significantly, and bring about a reduction in the potential at which the current reverses and becomes outward. Bassingthwaighte & Reuter (1972) attempted a study of the interrelationship between clamped membrane potential, observed i_s, and the apparent reversal potential. Their results indicate that the reversal potential for i_s is much less positive than would be predicted from a simple consideration of resting calcium levels in the muscle. Moreover, their results indicate a very rapid shift in reversal potential for calcium down to values as low as $+40$ mV within 20 msec of the application of a voltage-clamp step. In their discussion, Bassingthwaighte & Reuter (1972) postulated that the influx of calcium could be modelled to a first approximation by treating the calcium current as though it flowed into a volume of distribution that was only a few percent of total cell volume. They were not able, however, to precisely determine the resting level of the calcium concentration in that distribution space. In a recent study on calf ventricular trabeculae Reuter & Scholz (1976) have shown that the reversal potential, E_s, of i_s depends on the permeability ratio for calcium, sodium and potassium ions. The low E_s of less than $+40$ mV could be explained by a hundred times higher permeability of these conductance channels for calcium ions than for sodium or potassium ions. However, since the concentrations of sodium and potassium ions in the bulk solutions are much higher than those of calcium ions, a considerable fraction

of i_s is carried by the monovalent cations. This leads to a reversal potential of i_s which does not follow a simple Nernst relation. In calf trabeculae Reuter & Scholz (1976) have not observed major shifts of E_s during depolarizing clamp steps.

In order to produce a first approximation to the experimental results of Bassingthwaighte & Reuter (1972), we have chosen to model the intracellular handling of calcium as though it flows into a small distribution volume within the cell, from which it is removed by an uptake mechanism which will reduce the calcium concentration in that compartment exponentially with time to a level of 10^{-7} M. The rate constant for this uptake is set at 70 sec^{-1}. Thus the computer programme integrates the intracellular calcium ion concentration, utilizing eqn. (9) for the derivative. The reversal potential, E_s, is then calculated from $[Ca^{2+}]_i$ with the Nernst equation, as in eqn. (7). Although, as stated above, E_s is a mixed reversal potential, the use of eqn. (7) simplified our calculations.

The final element relative to calcium movement in the model is that of the fully activated conductance $\bar{g}_s$, which is on the order of 0·1 m-mho/cm^2 (Reuter & Scholz, 1976). The rate constant for uptake of calcium within the model was arrived at empirically by consideration of the plateau shape and of the over-all duration for the simulated action potential. The effects of modifications in the calcium handling system will be considered in the Results section.

Other currents

Earlier in this section it was indicated that at least four other current components have at one time or another been postulated to exist in cardiac muscle. These include a slow component of inward sodium current (Reuter, 1968), a dynamic chloride current (Dudel, Peper, Rüdel & Trautwein, 1967; Reuter, 1968; Fozzard & Hiraoka, 1973) and the two additional time varying outward currents (i_{K_2} and i_{x_2}; Noble & Tsien, 1968, 1969). The latter have been described clearly only for Purkinje fibres, and were discussed earlier. We have omitted the slow sodium current from this model because it is clear now that it is not a separable component of i_s (Vitek & Trautwein, 1971). The evidence for the dynamic inward movement of chloride is very strong in cardiac Purkinje fibres, but this current component does not appear to be present to any significant degree in ventricular myocardial preparations. In their report of the cardiac Purkinje fibre model, McAllister *et al.* (1975) note that the chloride current is required to produce a notch in the action potential, whereas our model exhibits such a notch without that component. If such a current is added to this model, its sole effect is to accentuate the notch between the spike of the action potential and the beginning of the plateau phase. This

discrepancy apparently results from the activation of i_s, which for inside positive potentials is at least twice as fast in the Purkinje fibre model as it is here. Moreover, the peak positive potential in their model is +40 mV as opposed to +28 mV in our model. The combined effect is that 12 msec into the action potential, where the minimum of the notch occurs, i_{si} in their model is virtually fully activated, while in this model, i_s is about half-activated at that time. Thus the notch in our model derives from the continued activation of i_s, superimposed on a relatively constant outward current, whereas in the Purkinje model it is the result of a transient repolarizing current component superimposed on a relatively constant inward current.

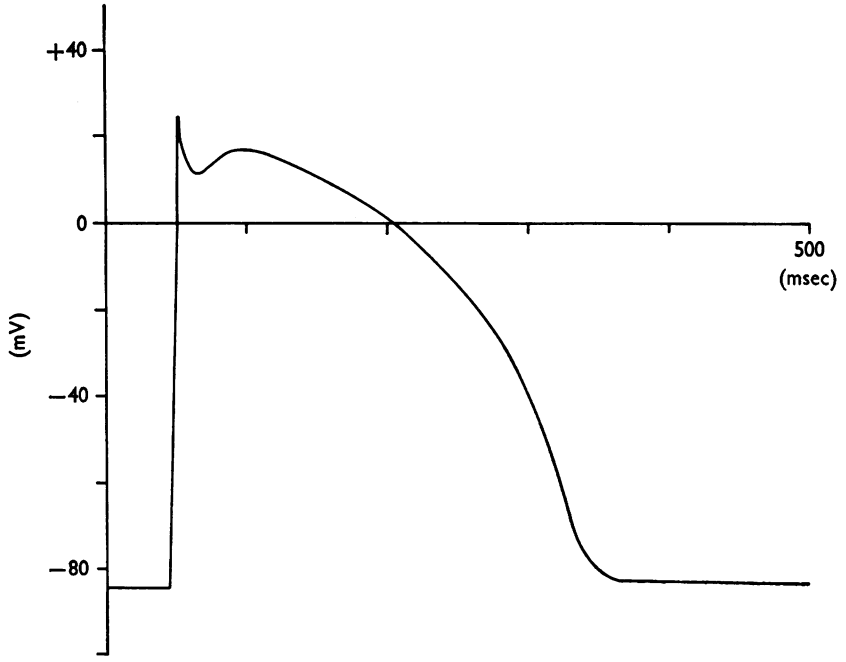

Fig. 4. The standard computed action potential (see text for details).

RESULTS

Action potential and V_{max}

The fundamental simulation produced by this model is the reproduction of a typical myocardial action potential as depicted in Fig. 4. The threshold is at −60 mV and the upstroke velocity of the action potential is 115 V/sec. After the initial spike the action potential reaches a maximum during the plateau phase of +17 mV and remains at inside positive potential levels for 153 msec. The maximum rate of repolarization is

about 1·1 V/sec, and the duration of the action potential measured at the point where re-polarization is 90 % complete is 285 msec. The resting potential is −84 mV.

One of the first questions pursued with the basic model was whether the altered formulation of i_{Na} did indeed match the experimental results of Gettes & Reuter (1974). One of the basic findings in their paper is the observation of two different curves for the rate of rise of the action potential as a function of starting potential, depending upon the method of measurement. If the conditioning depolarization which alters the rate of

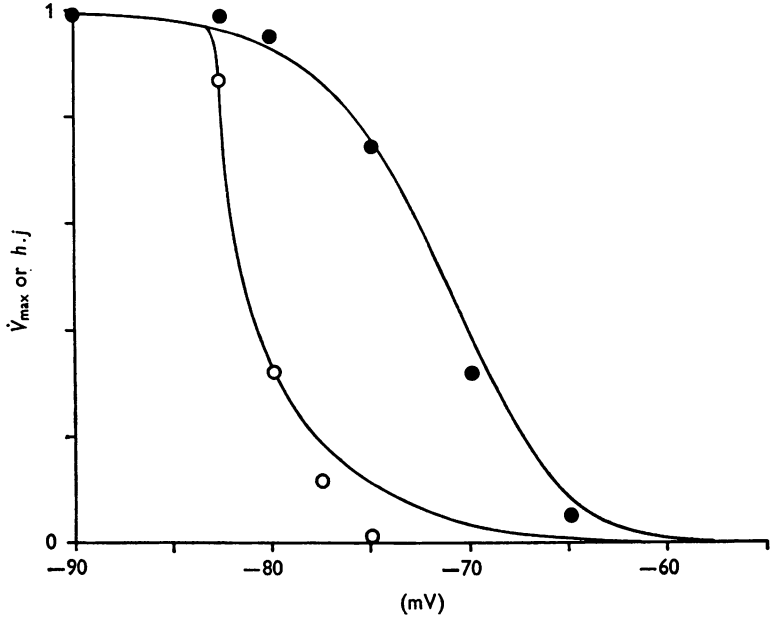

Fig. 5. Relative action potential upstroke velocity ($\dot{V}_{max}$), and product of Na inactivation variables ($h.j$) as functions of starting potential for two experimental simulations. Right-hand curve is the product of $h.j$ plotted with values of $\dot{V}_{max}$ (●) which result after a 500 msec conditioning clamp to voltage V_m. Left-hand curve is the inactivation product with $\dot{V}_{max}$ (○) values found when the stimulation is at different V_m during the re-polarization phase of a standard action potential.

rise of the action potential is accomplished with potassium chloride, or with a long-lasting voltage-clamp step, then the half-inactivation (V_h) of the upstroke of the cardiac action potential occurs in a potential range between 15 and 25 mV positive to the resting potential. If, on the other hand, an attempt is made to excite an action potential from a given membrane potential during the re-polarization phase of the preceding action potentials, which is often called 'membrane responsiveness' in the cardiac

muscle literature, the upstroke of the extrasystolic action potential is found to be half-inactivated at much more negative potentials. This difference is due to the fact that re-activation of i_{Na} is not an instantaneous function of the membrane potential. The simulation performed here involved the recreation of that basic experiment.

Two different sets of upstroke velocities were determined and are plotted in Fig. 5. For the first set, the membrane potential was pre-conditioned with a voltage-clamp step to various potential levels for 500 msec, and then released from clamp and stimulated. If the clamp duration is greater than τ_h, but less than τ_j, the observed maximum rate of rise of the action potential is related primarily to the inactivation curve, h_∞. If the clamp duration is greater than both τ_h and τ_j, as simulated here, the product of $h_\infty . j_\infty$ will govern V_{max}, but the result is very similar (see Discussion, p. 15). This has been confirmed with clamp durations as short as 50 msec where the observed velocities fall a few millivolts to the right of those plotted in Fig. 5 for 500 msec clamps. The alternative experiment is performed by allowing the membrane to re-polarize at the end of the action potential to the membrane potential desired, at which point the stimulation of a second action potential is attempted.

The measurements of Fig. 5 produce a picture similar to the experimental results of Gettes & Reuter (1974). In order to show more clearly the relationship between inactivation and the peak upstroke velocity in this experiment, we have also plotted the product of the inactivation variables, $h.j$, as a continuous function of V_m on the same graph. The observed velocity points fall close to these curves except for the points measured early in re-polarization. These are lower due to compounding factors such as i_{x_1} and $[Ca]_i$ which are elevated at this point in the action potential and which tend to further slow the observed rate of rise. It is clear from this Figure that the 'membrane responsiveness' curve utilizing the re-polarization of the preceding action potential to set the initial potential does not reflect the sodium inactivation curves in any meaningful way. Rather, it is dominated by the rate of re-polarization of the conditioning action potential and by the time that this allows the slow variable, j, to re-activate.

Determinants of action potential duration

One of the major questions which investigators have sought to resolve is which ionic current is primarily responsible for the determination of the duration of the myocardial action potential. This question is of interest because the influx of calcium during the action potential occurs primarily during the plateau phase, and hence the contractile state of the preparation will depend to a certain degree on action potential duration. In a

system such as that modelled here, the plateau phase of the action potential is determined by the antagonism between the outward currents, i_{K_1} and i_{x_1}, and the inward current, i_s. Thus, the termination of the plateau phase of the action potential could result from either the activation of i_{x_1} or the inactivation of i_s. Fig. 6 shows the values for the i_s inactivation parameter, f, and the i_{x_1} activation parameter, x_1, during the standard computed action potential. Clearly both of these parameters change

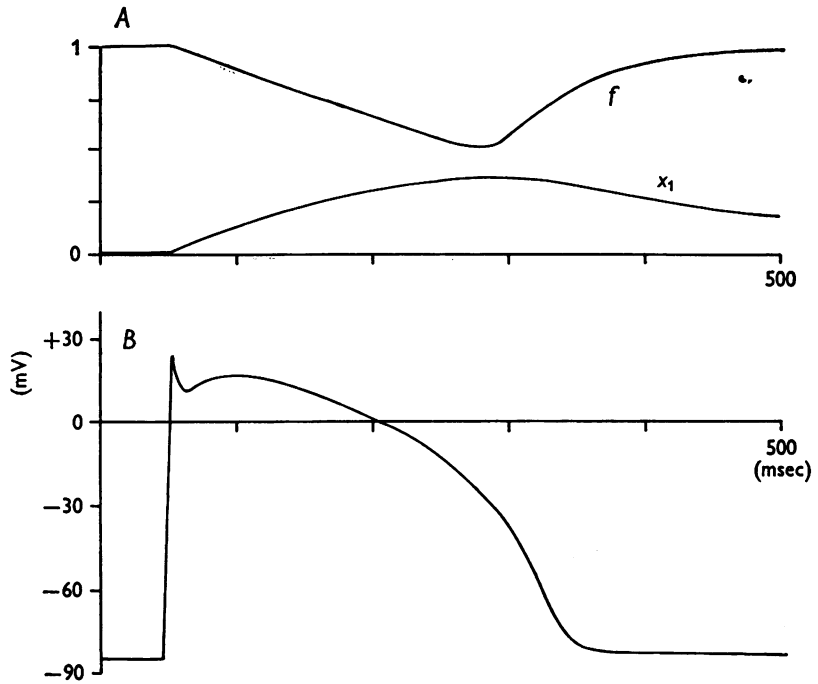

Fig. 6. *A*, variation of slow inward current inactivation parameter, f, and outward current activation parameter, x_1, during *B*, a standard action potential.

throughout the plateau phase of the action potential, although f undergoes a greater fractional change during the plateau than does x_1. The curves in Fig. 6 provide little insight into the question, however, as either mechanism might be deemed responsible. Giebisch & Weidmann (1971) studied this question in sheep ventricular trabeculae using a voltage-clamp, and concluded that the decline of the inward current was the dominant factor. Similar conclusions were reached by Beeler & Reuter (1970*b*), New & Trautwein (1972), and Reuter & Scholz (1976). McAllister *et al.* (1975), however, conclude that the activation of i_{x_1} is more important in cardiac Purkinje fibres.

Given that our model is an admixture of results obtained from Purkinje fibres for the outward currents, and from ventricular myocardium for the inward current, we sought to gain further insight from experimentation on the model. One way of doing this is to produce systematic alterations of the individual ionic currents. The two panels of Fig. 7 show results of

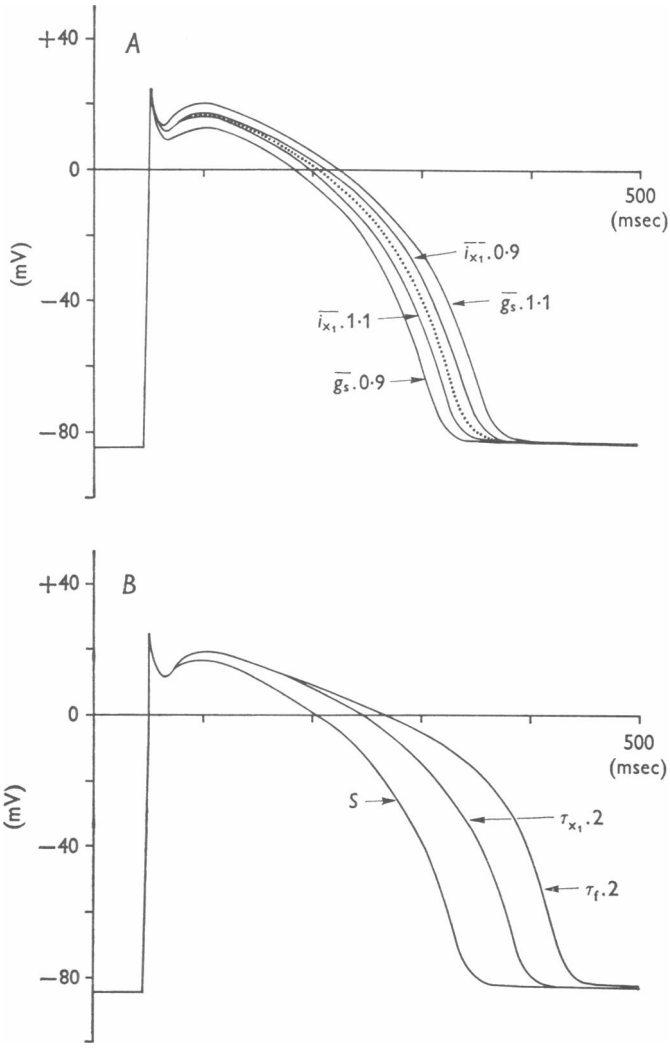

Fig. 7. The effects of altering i_s and i_{x_1} parameters. *A*, five action potentials showing the relative effects of altering the fully activated currents for i_{x_1} and i_s by $\pm 10\,\%$. The greater change is caused by alterations of i_s. *B*, three action potentials showing the effect of increasing the time constants for x_1 and f by factors of 2. Slowing the inactivation of i_s produces the greater changes. (Standard action potential indicated by *S*.)

such alterations. In the first instance (Fig. 7*A*), the fully activated current values for i_{x_1} and for i_s were changed by $+10\%$ individually. A 10% change in $\overline{g_s}$ produces a larger alteration in action potential duration, than does an equivalent change in $\overline{i_{x_1}}$. Alternatively, one can change the time constant for the two parameters in question. In Fig. 7*B* are shown the action potentials which result when the time constants for f and x_1 are individually increased by a factor of two. Again, the duration of the action potential is significantly more sensitive to an alteration in i_s inactivation time than it is to an equivalent alteration in i_{x_1} activation time.

Although these results might argue for the decline in i_s being the dominant factor in action potential length, we have also considered the question of the effect of the larger time constant for x_1 at the resting potential (233 msec) compared to that for f at that potential (54 msec). The shortening of the action potentials which occurs when the stimulus frequency is increased or when extrasystoles are interpolated within a train of action potentials at constant frequency is a well known phenomenon, and is reproduced by this model. As the time interval between action potentials is decreased, the variables x_1 and f have less time to recover (deactivate and re-activate, respectively). Thus, at the start of the action potential in question, i_{x_1} is already partially activated, and i_s is already partially inactivated. Both effects will shorten the action potential, but presumably the i_{x_1} effect may dominate since its longer time constant will permit less recovery.

In order to test this presumption, we stimulated the model action potential at various frequencies between 1 and 4/sec, and interpolated extrasystoles at intervals from 667 msec down to 300 msec into a steady 1/sec train. As expected, the action potential duration decreases as the proximity to the preceding action potential gets smaller. Moreover, the change in duration begins to occur at the proximity where x_1 begins to build up, thus confirming the presumption that activation of x_1 is important for action potential shortening in this case even though the duration decreases most drastically when f decreases. These results obtained with the model action potential are very similar to those obtained experimentally by Gettes, Morehouse & Surawicz (1972).

In the process of questioning the relative importance of the inward and outward currents for re-polarization, we have also sought a simple experiment that might be applied to any cardiac tissue in order to assess the roles of these currents. Kass & Tsien (1976) and Reuter & Scholz (1976) have suggested that a pulse of depolarizing current applied during the early stages of the action potential ought to separate the effects. If i_{x_1} predominates, the added depolarization from such a current should increase the activation of x_1 and thus shorten the action potential. If i_s is

dominant, on the other hand, the long time constants for f at inside positive potentials will mean that the inactivation of i_s will be little changed, and the action potential may then be prolonged by the prolonged depolarization produced by the test current.

Fig. 8*A* shows an experimental test of this hypothesis on Purkinje fibres and on ventricular myocardium from calf hearts. The Purkinje

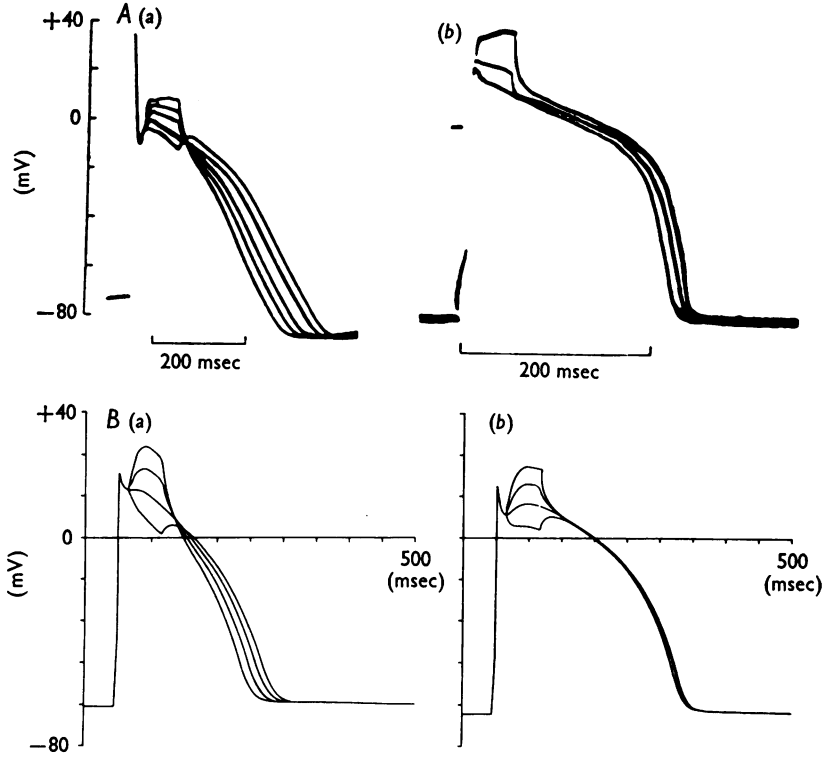

Fig. 8. *A*, superimposed action potentials recorded from (*a*) a calf Purkinje fibre and (*b*) a calf ventricular trabecula in Tyrode solution. Note *shortening* of the action potential duration after application of constant depolarizing current pulses at the beginning of the plateau phase in case of the Purkinje fibre (from Kass & Tsien, 1976) and modest *lengthening* in case of the ventricular trabeculae (H. Reuter, unpublished). *B*, corresponding reconstructions. (See text for details.)

fibre result (Kass & Tsien, 1976), a shortening of the action potential after depolarizing current pulses at the beginning of the plateau, is as one would expect from the model of McAllister *et al.* (1975), while the ventricular myocardial preparation shows a modest prolongation of the action potential under similar conditions indicating less influence of time-activated outward current. Our own experiments in dog (Beeler & Reuter, 1970*a*),

sheep, calf and cat hearts (Gettes & Reuter, 1974; Reuter & Scholz, 1976) confirm the species difference in time-activated outward current, this current being larger in dog and cat than in sheep or calf ventricular fibres. Fig. 8*B* is a simulation of two ventricular myocardium experiments. The right-hand panel (*a*) is our standard reconstruction which shows virtually no effect of the imposed current pulses on the action potential duration. The left-hand panel (*b*) represents a modified model which may be more closely applicable to myocardial fibres with large i_{x_1} and which mimics the Purkinje fibre results in Fig. 8*A* (see also Kass & Tsien, 1976, Fig. 4*C*). In this modified model, the relative importance of i_s and i_{x_1} for re-polarization was reversed by reducing $\overline{g_s}$ to two thirds its normal value, and increasing i_{x_1} to twice normal. In order to retain a normal spike and early plateau, i_{K_1} was also reduced to one half normal. Oppositely directed changes in the same parameters produce a model which shows clear prolongation of the action potential when depolarizing currents are applied, confirming that this simple experiment will demonstrate the relative dependence of action potential duration upon these two currents.

All-or-nothing re-polarization

One of the experimental methods that has been used in the past to characterize the plateau phase of the cardiac action potential, is to attempt to force premature re-polarization of the action potential by applying a constant current stimulus during the plateau phase of the action potential (Weidmann, 1951). This procedure generally shows that premature re-polarization will occur if the current drops the membrane potential below a threshold level, and that this threshold is at progressively more positive potentials later in the action potential (Vassalle, 1966). In the process of investigating this experiment with the model, we altered the experimental method by imposing a brief voltage clamp during the action potential (Fig. 9). When such a clamp is imposed either experimentally or on the model, a decaying tail of inward current is observed if the membrane potential during the clamp is more negative than the normal action potential level. If the voltage-clamp is released at a time when the current tail is still inward, the membrane will tend to depolarize a second time and follow its normal course of re-polarization. Otherwise, i.e. if the net current is outward, the membrane potential will re-polarize prematurely. Examples of these phenomena in the model are given in the four panels of Fig. 10. Here, voltage-clamps have been imposed at various intervals of delay after the stimulus to the action potential, and held for varying times. Analysis of these data shows that the duration of the clamp needed to force premature re-polarization at any given potential level is directly related to the time constant for the activation parameter, τ_d, for i_s at that

potential level. Thus the clamp brings about a reduction in inward current by deactivation of i_s. If this process is not completed before the time when the membrane potential is released from clamp, then i_s re-activates and produces a second depolarization to potential levels equal to or beyond those which would be achieved by the normal action potential. This can be seen most clearly in Fig. 9 *C* and Fig. 10 *D*. The interaction between the

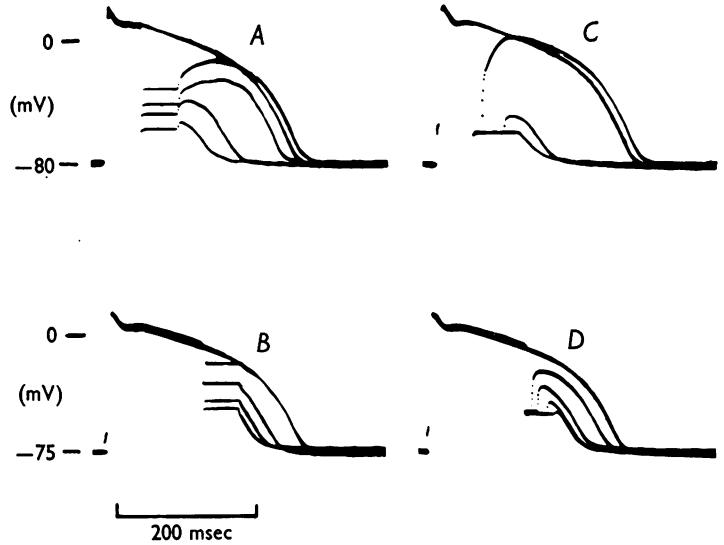

Fig. 9. All-or-nothing re-polarization in a dog ventricular trabecula: *A*, *C*, hyperpolarizing clamp steps applied 50 msec or *B*, *D*, 120 msec after the beginning of the action potential; *A*, *B*, clamp steps (50 msec duration) to different potential levels, or *C*, *D*, for different times (10–60 msec duration; all-or-nothing response is best illustrated in *C*.

on-going inactivation of i_s and the activation of i_{x_1} brings about a steadily higher potential level at which a clamp of any given duration will bring about all-or-nothing re-polarization. This can be seen by comparing the voltage levels at which the action potential repolarizes prematurely in *A*–*C* of Fig. 10 (cf. Fig. 9*A*, *B*), and agrees with the experimental reports of Vassalle (1966), Reuter & Beeler (1971), and McAllister *et al.* (1975).

Oscillatory potentials

Although the electrical characteristics of the working myocardium are such that these preparations seldom produce spontaneous activity, numerous experimental conditions have been created where such observations can be made. Reuter & Scholz (1968) found that preparations in a low sodium, high calcium medium produced membrane potential oscillations when depolarized with outward current. More recently, Katzung

(1975) has reported a series of experiments on ventricular myocardial preparations in a sucrose gap, wherein a steady depolarizing current brings about oscillatory potentials in working myocardium in the absence of any other ionic or pharmacologic intervention. This mechanism can be readily simulated in the model as seen in Fig. 11 which shows the model response to two different steady depolarizing currents. At a moderate depolarization a stable oscillation of about one every 1·3 sec results. At

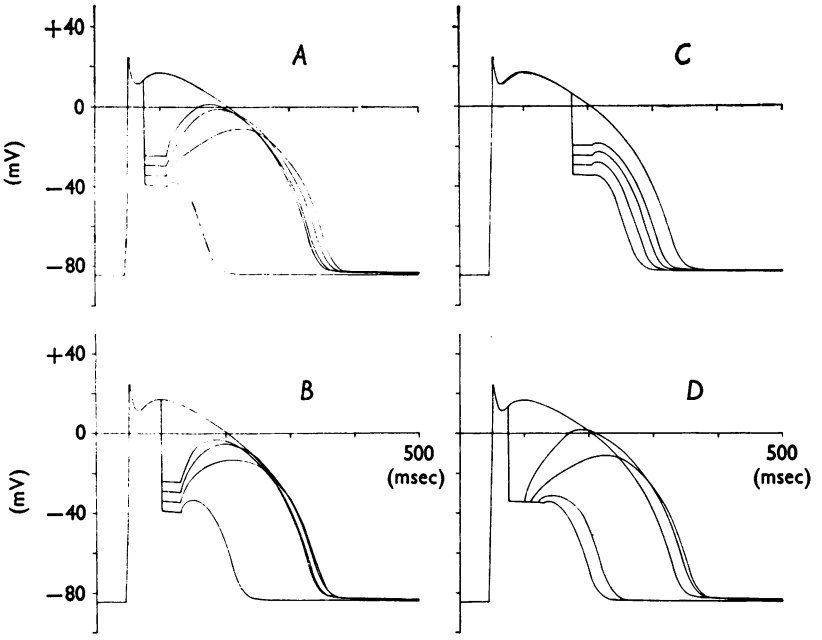

Fig. 10. All-or-nothing re-polarization induced by voltage-clamps imposed during the plateau of a simulated action potential. *A*, voltage-clamps commence 25 msec after the stimulus, last for 35 msec, and are at levels of −25, −30, −35, and −40 mV. *B*, clamps are 35 msec duration, are imposed 75 msec after the stimulus, and are at voltage levels of −25, −30, −35 and −40 mV. *C*, voltage-clamps are 30 msec duration, imposed 125 msec after stimulus, at voltage levels −20, −25, −30, and −35 mV. *D*, effects of varying the duration of voltage-clamps which start 25 msec after the stimulus at the −35 mV level; durations are 25, 35, 45 and 55 msec.

still larger depolarizations, the model exhibits a damped oscillation around a stable potential level at −20 mV. These results match quite well the experimental findings by Reuter & Scholz (1968) and by Katzung (1975).

The two panels of Fig. 12 show the ionic current dependencies of this oscillatory behaviour of the membrane. Fig. 12*A* shows two tracings

created with a steady current of 2·1 μA/cm^2. The earlier tracing is the basic model, while the later tracing was simulated with the conductance for the sodium current, $\overline{g_{Na}}$, set to zero such as might occur in the presence of tetrodotoxin or in Na-free solution (Katzung, 1975; Reuter & Scholz,

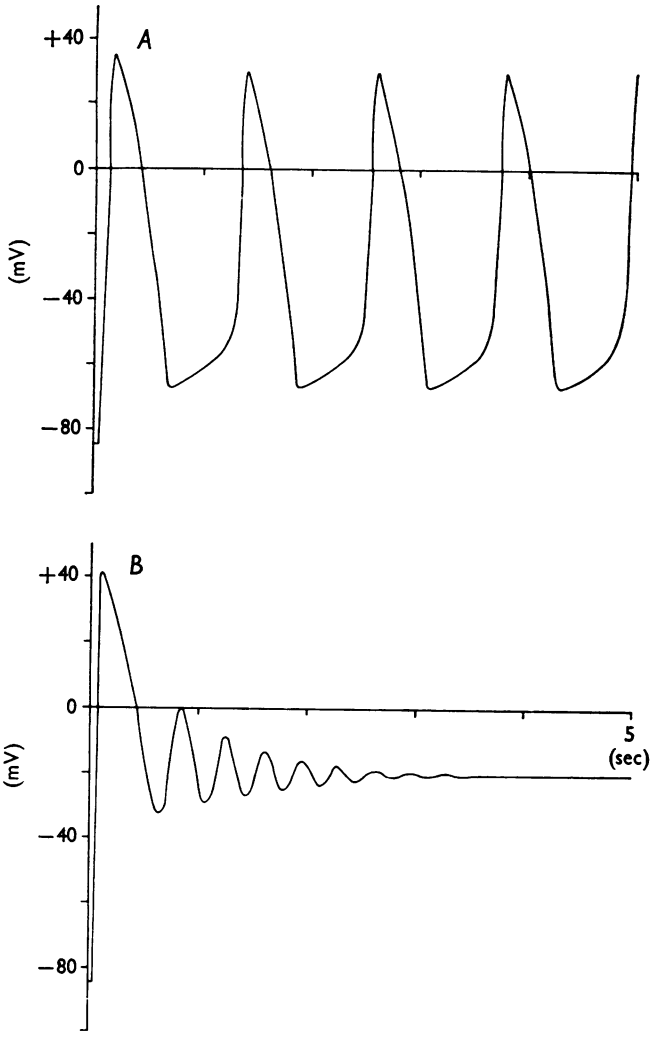

Fig. 11. Oscillatory potentials created with steady outward currents of: *A*, 2·3 μA/cm^2 and *B*, 2·8 μA/cm^2.

1968). The depolarization of the earliest action potential is brought about by the active sodium system in the standard model. The subsequent repolarization, however, does not proceed to sufficiently negative values

to allow the re-activation of the sodium system. Thus the second and subsequent oscillations brought about by the steady outward current produce virtually identically shaped action potentials for the two reconstructions, and the only difference in the action potential trains observed is the time delay created at the occurrence of the first action potential.

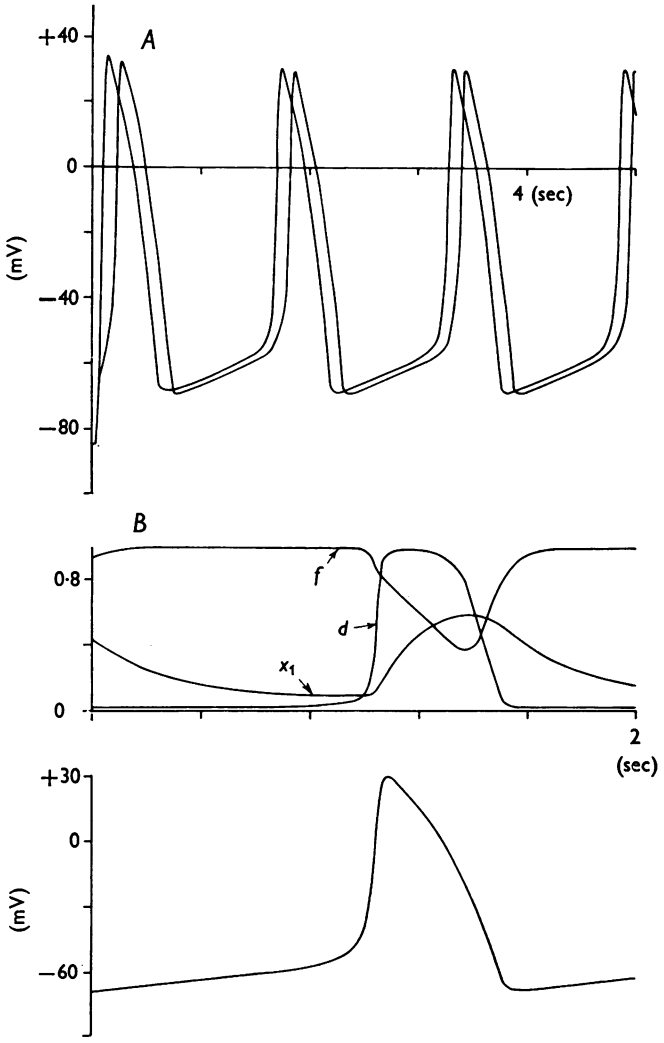

Fig. 12. *A*, effect on the oscillatory potentials of eliminating the dynamic sodium inward current, i_{Na}. The earlier tracing is normal model, the later one is model without i_{Na}. *B*, membrane potential and kinetic parameters observed during a single cycle of *A*. Activation and inactivation parameters for i_s, d and f, and i_{x_1} activation parameter, x_1, are plotted above the oscillatory membrane potential.

Since Fig. 12*A* demonstrates that the oscillatory behaviour is not a phenomenon which depends on $\overline{g_{Na}}$, it is of interest to investigate further the ionic conductance mechanisms responsible for this oscillation. Fig. 12*B* shows a single cycle of the oscillations from the upper panel plotted along with the values for the conductance parameters which moderate i_s and i_{x_1}. During the slow depolarization phase the change in membrane potential results from a slow decay of the x_1 outward current. At about -40 mV, i_s is progressively activated bringing about an increasing speed of depolarization of the membrane. Subsequently, the combined factors of the inactivation of i_s and the activation i_{x_1} bring about repolarization to about -70 mV. Thus this oscillatory behaviour is a 'slow response' dependent on i_s. As a final note, oscillatory behaviour of the sort shown here can be readily produced in the model in the absence of a stimulus by simply increasing the leak conductance to sodium, $\overline{g_{NaC}}$, eightfold.

Calcium mechanisms

A common finding in cardiac electrophysiology is a shortening of the action potential duration with increasing extracellular calcium ion concentration. On face value, one might expect that the calcium inward current would be increased in this situation, owing to an increased driving force, and ought to bring about an increase in action potential duration. This, however, is seen only at very low rate of stimulation ($<0{\cdot}1$ Hz; Niedergerke & Orkand, 1966; Bassingthwaighte, Fry & McGuigan, 1976), while at higher driving rates the action potential duration shortens. The reason for this apparent discrepancy, however, is probably a secondary effect of the change in extracellular and intracellular calcium ion concentration on the conductance of the membrane to potassium ions. Recent reports by Meech (1972) working with *Aplysia* neurones, by Isenberg (1975) in cardiac Purkinje fibres and by Bassingthwaighte *et al.* (1976) in ventricular myocardium demonstrate that membrane conductance to potassium can be significantly and rapidly altered by an alteration in the intracellular calcium ion concentration. Moreover, one of the effects of an increase in the extracellular calcium ion concentration in addition to increasing i_s will be to bring about an increase in the intracellular calcium concentration via the Na–Ca exchange mechanism (Reuter & Seitz, 1968) studied in various excitable tissues (for references see Blaustein, 1974). Therefore in simulating the effects of an increase in extracellular calcium ion concentration, one ought also to make a concomitant change in the formulation for the potassium currents. An example of the attempt to simulate such behaviour is seen in Fig. 13. Here, the effects of producing *e*-fold changes in the extracellular calcium ion concentration are modelled by three changes in the basic model parameters. Firstly, the reversal

potential computation for i_s is altered in order to recognize the change in the Nernst relationship brought about by the increase or decrease in extracellular calcium concentration, $[Ca]_o$. Secondly, all potassium current components in the model are altered by 15 % in the same direction as the change in $[Ca]_o$. Thirdly, altering $[Ca]_o$ will change the external surface charge of the membrane and will result in a shift along the voltage axis

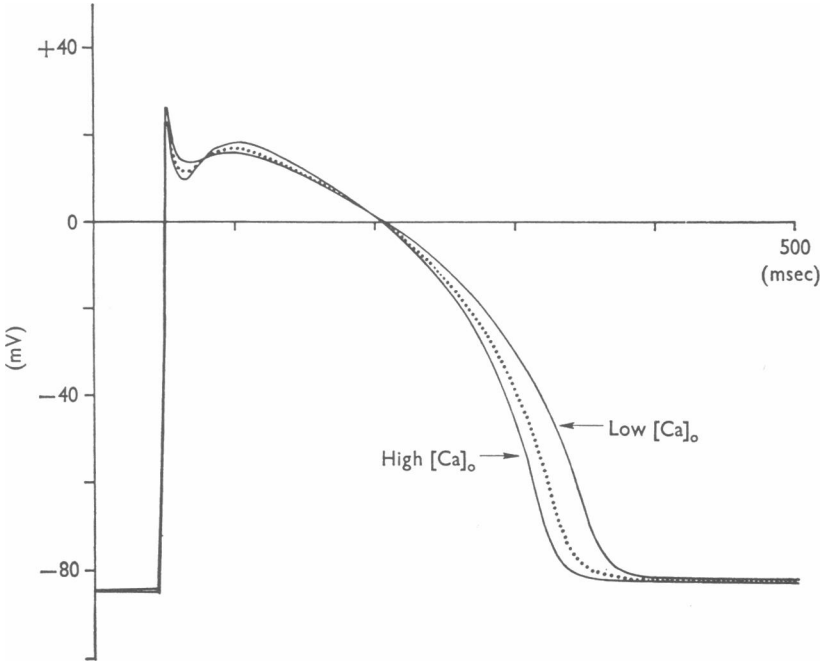

Fig. 13. Simulation of the effects of an *e*-fold increase or decrease in the extracellular calcium ion concentration; plotted along with standard reconstruction (dotted line). See text for details of model alterations.

of all conductance parameters (Frankenhaeuser & Hodgkin, 1957; Weidmann, 1955*b*; Reuter & Scholz, 1976). In our model, an *e*-fold increase in $[Ca]_o$ shifts all conductance parameters by 4 mV in the depolarizing direction on the voltage axis. The resulting action potentials (Fig. 13) demonstrate the characteristic change in action potential duration that is seen with such an experimental intervention. Although i_s is indeed larger and results in a higher plateau in the instance of increased $[Ca]_o$, the concomitant increase in potassium conductance brings about an earlier re-polarization of the membrane potential. Moreover, the effect of i_s on the plateau is accentuated by the shift in conductance parameters, and the latter intervention alters the threshold of the rapid upstroke of the action potential, increasing the threshold with increasing $[Ca]_o$.

An increase in i_{K_1} due to accumulation of $[Ca]_i$ (Bassingthwaighte *et al.* 1976) and accumulation of $[K]_o$ (Cleemann & Morad, 1976) may also contribute to the shortening of the action potential during rapid stimulation.

As was noted earlier, one of the greatest uncertainties in defining the calcium conductance was the formulation of the intracellular handling of calcium. The model adopted here proposes that the calcium current flows into a limited volume within the cell, and then is sequestered from this volume by some intracellular process, probably the sarcoplasmic

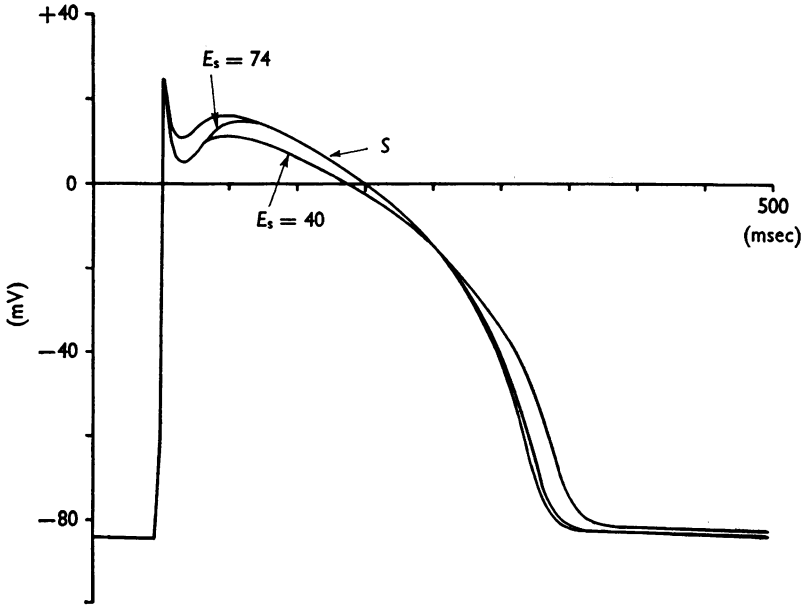

Fig. 14. Effect on the simulated action potential of forcing constant reversal potential E_s at 74 mV, and 40 mV, along with standard simulation, S. (See text for discussion.)

reticulum (for further discussion of this see Bassingthwaighte & Reuter, 1972). One of the questions which we have sought to address with the model is the effect upon the computed action potential of these assumptions. Alterations in the parameters which define this process have predictable effects. Thus, increasing the volume of distribution brings about a lesser reduction in calcium reversal potential. The increased i_s, which results from the increased driving force, produces a higher plateau and longer action potential. Similar changes result if the rate constant at which calcium is removed from this volume is increased. Of greater interest, however, is the effect of keeping E_s constant. Fig. 14 shows two such models along with the standard reconstruction. In the first, E_s is

held fixed at 74 mV, the level reached during the plateau of normal reconstruction. This version deviates from the standard tracing only during the early plateau phase, where E_s in the standard reconstruction is changing most rapidly.

The second altered reconstruction has E_s fixed at 40 mV (Reuter & Scholz, 1976). In this reconstruction $\overline{g_s}$ and i_{x_1} are multiplied by 2·2 and 1·9 respectively, to arrive at approximately the same shape action potential. Again, there is little qualitative difference between this reconstruction and the standard version. Indeed, all of the phenomena discussed earlier in the paper can be reproduced on any of these versions.

DISCUSSION

The main object of this paper has been the reconstruction of an action potential of mammalian ventricular myocardium on the basis of ionic currents measured in voltage-clamp experiments. Most of the detailed properties of this model have been discussed in the Results. Hence it remains to emphasize briefly some major features and shortcomings of our reconstruction.

The membrane action potential model is based on two inward and two outward current systems for which experimental evidence is available. However, for the reconstruction of propagated action potentials it would be desirable to have more detailed information about the kinetic properties of the excitatory i_{Na}. Unfortunately, none of the published voltage-clamp methods applied to cardiac muscle are adequate to provide this information. Here we see one of the major shortcomings of our model, since it does not predict action potential behaviour during conduction or conduction disturbances, e.g. during arrhythmias.

The other ionic currents, i_s, i_{K_1} and i_{x_1}, are defined experimentally much better than i_{Na}. Therefore it is not surprising that features of the cardiac action potential which depend on these current components are simulated quite well by our reconstruction. Re-polarization of the action potential is induced by the time-dependent decrease of the slow inward current, i_s, and by the increase of the time-dependent outward current, i_{x_1}. The relative contribution of both current components to re-polarization depends on the animal species and on the experimental conditions. In most instances the decrease of i_s seems to be the dominant factor. However, particularly during fast repetitive stimulation the build-up of i_{x_1} becomes important for the shortening of the action potential duration.

The model simulates rather successfully 'all-or-nothing re-polarization' as well as the prolongation of the action potential after depolarizing current pulses during the plateau. These features are primarily dependent on

the kinetic properties of i_s. The close agreement between experimental results and computer reconstruction suggests that our model describes these kinetics quite accurately.

A very intriguing phenomenon is the oscillatory behaviour of the membrane potential during application of a constant outward current. Such oscillations were first described by Reuter & Scholz (1968) in ventricular trabeculae superfused with sodium-free solution. Our reconstruction model simulates these oscillations and confirms its independence of i_{Na} and its dependence on i_s and i_{x_1}. Such pace-maker activity may be of importance for generation of ectopic pace-makers in cardiac arrhythmias. It has also been suggested that 'slow responses' which depend on i_s are important for re-entrant arrhythmias (Cranefield, 1975).

A subject of major experimental uncertainty is whether and under which conditions extracellular and intracellular accumulation, or depletion, or both, of ions may occur. In our model we have incorporated only a rapid and transient accumulation of intracellular calcium ions. However, other changes in local ion concentrations may occur during normal or pathologically altered action potentials. Thus, extracellular accumulation of potassium ions has been observed under experimental conditions in frog and mammalian ventricle (Cleemann & Morad, 1976; McGuigan, 1974). Such shifts in ion concentrations, if they occur *in vivo* in the whole heart, may be responsible for local changes in the shape of the action potential which, in turn, should be reflected by the electrocardiogram.

A more complete model of the cardiac action potential than ours will also have to include current components generated by electrogenic pump mechanisms. It will be interesting to see how the inclusion of such mechanisms will alter the basic properties of our action potential model.

This work has been supported by grants HL 12824 and RR 00007 of the U.S. National Institutes of Health and by grants 3.734.72 and 3.598.75 of the Swiss National Science Foundation. This work was performed during the tenure of an Established Investigatorship of the American Heart Association (G.W.B.).

REFERENCES

ANDERSON, D. U., KNOPP, T. J. & BASSINGTHWAIGHTE, J. B. (1970). SIMCON-Simulation control to optimize man-machine interaction. *Simulation* **14**, 81–86.

BASSINGTHWAIGHTE, J. B., FRY, C. H. & MCGUIGAN, J. A. S. (1976). Relationship between internal calcium and outward current in mammalian ventricular muscle; a mechanism for the control of the action potential duration? *J. Physiol.* **262**, 15–37.

BASSINGTHWAIGHTE, J. B. & REUTER, H. (1972). Calcium movements and excitation contraction coupling in cardiac cells. In *Electrical Phenomena in the Heart*, ed. DE MELLO, W. C., pp. 353–395. New York: Academic Press.

BEELER, G. W., JR & REUTER, H. (1970*a*). Voltage clamp experiments on ventricular myocardium fibres. *J. Physiol.* **207**, 165–190.

BEELER, G. W., JR & REUTER, H. (1970*b*). Membrane calcium current in ventricular myocardium fibres. *J. Physiol.* **207**, 191–209.

BLAUSTEIN, M. P. (1974). The interrelationship between sodium and calcium fluxes across cell membranes. *Rev. Physiol. Biochem. Pharmac.* **70**, 34–82.

CLEEMANN, L. & MORAD, M. (1976). Extracellular potassium accumulation and inward-going potassium rectification in voltage clamped ventricular muscle. *Science, N.Y.* **191**, 90–92.

CRANEFIELD, P. F. (1975). *The Conduction of the Cardiac Impulse.* Mount Kisco, N.Y.: Futura.

DUDEL, J., PEPER, K., RÜDEL, R. & TRAUTWEIN, W. (1967). The dynamic chloride component of membrane current in Purkinje fibres. *Pflügers Arch. ges. Physiol.* **295**, 197–212.

FRANKENHAEUSER, B. & HODGKIN, A. L. (1957). The action of calcium on the electrical properties of squid axons. *J. Physiol.* **137**, 218–244.

FOZZARD, H. A. & HIRAOKA, M. (1973). The positive dynamic current and its inactivation properties in cardiac Purkinje fibres. *J. Physiol.* **234**, 569–586.

GETTES, L. S., MOREHOUSE, N. & SURAWICZ, B. (1972). Effect of premature depolarization on the duration of action potentials in Purkinje and ventricular fibres of the moderator band of the pig heart. Role of proximity and the duration of the preceding action potential. *Circulation Res.* **30**, 55–66.

GETTES, L. S. & REUTER, H. (1974). Slow recovery from inactivation of inward currents in mammalian myocardial fibres. *J. Physiol.* **240**, 703–724.

GIEBISCH, G. & WEIDMANN, S. (1971). Membrane currents in mammalian ventricular heart muscle fibres using a voltage-clamp technique. *J. gen. Physiol.* **57**, 290–296.

GOLDMAN, L. (1975). Quantitative description of the sodium conductance of the giant axon of *Myxicola* in terms of a generalized second order variable. *Biophys. J.* **15**, 119–136.

HAAS, H. G., KERN, R. EINWÄCHTER, H. M. & TARR, M. (1971). Kinetics of Na inactivation in frog atria. *Pflügers Arch. ges. Physiol.* **323**, 141–157.

HODGKIN, A. L. & HUXLEY, A. F. (1952). A quantitative description of membrane current and its application to conduction and excitation in nerve. *J. Physiol.* **117**, 500–544.

ISENBERG, G. (1975). Is potassium conductance of cardiac Purkinje fibres controlled by $[Ca^{2+}]_i$? *Nature, Lond.* **253**, 273–274.

KASS, R. S. & TSIEN, R. W. (1976). Control of action potential duration by calcium ions in cardiac Purkinje fibres. *J. gen. Physiol.* **67**, 599–617.

KATZUNG, B. G. (1975). Effects of extracellular calcium and sodium on depolarization-induced automaticity in guinea pig papillary muscle. *Circulation Res.* **37**, 118–127.

KOHLHARDT, M., KRAUSE, J., KÜBLER, M. & HERDEY, A. (1975). Kinetics of inactivation and recovery of the slow inward current in the mammalian ventricular myocardium. *Pflügers Arch. ges. Physiol.* **355**, 1–17.

LANGE, G. E. (1960). *Numerical Methods for High Speed Computers*, pp. 54–57. London: Iliffe.

MCALLISTER, R. E., NOBLE, D. & TSIEN, R. W. (1975). Reconstruction of the electrical activity of cardiac Purkinje fibres. *J. Physiol.* **251**, 1–59.

MCGUIGAN, J. A. S. (1974). Some limitations of the double sucrose gap and its use in a study of the slow outward current in mammalian ventricular muscle. *J. Physiol.* **240**, 775–806.

MEECH, R. W. (1972). Intracellular calcium injection causes increased potassium conductance in *Aplysia* nerve cells. *Comp. Biochem. Physiol.* **42A**, 493–499.

NEW, W. & TRAUTWEIN, W. (1972). Inward membrane currents in mammalian myocardium. *Pflügers Arch. ges. Physiol.* **334**, 1–23.

NIEDERGERKE, R. & ORKAND, R. K. (1966). The dual effect of calcium on the action potential of the frog's heart. *J. Physiol.* **184**, 291–311.

NOBLE, D. (1975). *The Initiation of the Heart Beat.* Oxford: Clarendon Press.

NOBLE, D. & TSIEN, R. W. (1968). The kinetics and rectifier properties of the slow potassium current in cardiac Purkinje fibres. *J. Physiol.* **195**, 185–214.

NOBLE, D. & TSIEN, R. W. (1969). Outward membrane currents activated in the plateau range of potentials in cardiac Purkinje fibres. *J. Physiol.* **200**, 205–232.

REUTER, H. (1968). Slow inactivation of currents in cardiac Purkinje fibres. *J. Physiol.* **197**, 233–253.

REUTER, H. (1973). Divalent cations as charge carriers in excitable membranes. *Prog. Biophys. molec. Biol.* **26**, 1–43.

REUTER, H. (1974). Localization of beta adrenergic receptors and effects of noradrenaline and cyclic nucleotides on action potentials, ionic currents and tension in mammalian cardiac muscle. *J. Physiol.* **242**, 429–451.

REUTER, H. & BEELER, G. W., JR (1971). The mechanism of all-or-nothing repolarization in ventricular myocardial fibres. *Proc. int. Union Physiol. Sci.* **9**, 472.

REUTER, H. & SCHOLZ, H. (1968). Über den Einfluss der extracellularen Ca-Konzentration auf Membranpotential und Kontraktion isolierter Herzpräparate beigraduierter Depolarisation. *Pflügers Arch. ges. Physiol.* **300**, 87–107.

REUTER, H. & SCHOLZ, H. (1976). A study of the ion selectivity and the kinetic properties of the calcium-dependent slow inward current in mammalian cardiac muscle. *J. Physiol.* **264**, 17–47.

REUTER, H. & SEITZ, N. (1968). The dependence of calcium efflux from cardiac muscle on temperature and external ion composition. *J. Physiol.* **195**, 451–470.

TRAUTWEIN, W. (1973). Membrane currents in cardiac muscle fibers. *Physiol. Rev.* **53**, 793–835.

TRAUTWEIN, W., MCDONALD, T. F. & TRIPATHI, O. (1975). Calcium conductance and tension in mammalian ventricular muscle. *Pflügers Arch. ges. Physiol.* **354**, 55–74.

VASSALLE, M. (1966). Analysis of cardiac pacemaker potential using a 'voltage-clamp' technique. *Am. J. Physiol.* **210**, 1335–1341.

VITEK, M. & TRAUTWEIN, W. (1971). Slow inward current and action potential in cardiac Purkinje fibres. The effect of Mn^{++} ions. *Pflügers Arch. ges. Physiol.* **323**, 204–218.

WEIDMANN, S. (1951). Effect of current flow on the membrane potential of cardiac muscle. *J. Physiol.* **115**, 227–236.

WEIDMANN, S. (1955*a*). The effect of the cardiac membrane potential on the rapid availability of the sodium carrying system. *J. Physiol.* **127**, 213–224.

WEIDMANN, S. (1955*b*). Effects of calcium ions and local anaesthetics on electrical properties of Purkinje fibres. *J. Physiol.* **129**, 568–582.

WEIDMANN, S. (1970). Electrical constants of trabecular muscle from mammalian heart. *J. Physiol.* **210**, 1041–1054.